A novel slow hyperpolarization-activated potassium current ($I_{K(SHA)}$) from a mouse hippocampal cell line

Erhard Wischmeyer and Andreas Karschin *

Max-Planck-Institute for Biophysical Chemistry, Molecular Neurobiology of Signal Transduction, Am Fassberg 11, D-37070 Göttingen, Germany

1. A slow hyperpolarization-activated inwardly rectifying K^+ current ($I_{K(SHA)}$) with novel characteristics was identified from the mouse embryonic hippocampus × neuroblastoma cell line HN9.10e.

2. The non-inactivating current activated negative to a membrane potential of −80 mV with slow and complex activation kinetics ($\tau_{act} \approx 1$–7 s) and a characteristic delay of 1–10 s (−80 to −140 mV) that was linearly dependent on the membrane potential.

3. Tail currents and instantaneous open channel currents determined through fast voltage ramps reversed at the K^+ equilibrium potential (E_K) indicating that primarily K^+, but not Na^+, permeated the channels.

4. $I_{K(SHA)}$ was unaffected by altering the intracellular Ca^{2+} concentration between ~0 and 10 μM, but was susceptible to block by 5 mM extracellular Ca^{2+}, Ba^{2+} ($K_i = 0{\cdot}42$ mM), and Cs^+ ($K_i = 2{\cdot}77$ mM)

5. In cells stably transformed with M2 muscarinic receptors, $I_{K(SHA)}$ was rapidly, but reversibly, suppressed by application of micromolar concentrations of muscarine.

6. At the single channel level K(SHA) channel openings were observed with the characteristic delay upon membrane hyperpolarization. Analysis of unitary currents revealed an inwardly rectifying *I–V* profile and a channel slope conductance of 7 pS. Channel activity persisted in the inside-out configuration for many minutes.

7. It is concluded that $I_{K(SHA)}$ in HN9.10e cells represents a novel K^+ current, which is activated upon membrane hyperpolarization. It is functionally different from both classic inwardly rectifying I_{Kir} currents and other cationic hyperpolarization-activated I_H currents that have been previously described in neuronal or glial cells.

When engineering clonal cell lines from the central nervous system, oncogenic DNA has to be stably introduced via viral vectors into immature cells still capable of dividing, but somatic cell fusion permits the immortalization of postmitotic cells that are more likely to express the properties of differentiated cells (Lee *et al.* 1990). HN9.10e cells are a somatic fusion product of hippocampal cells from embryonic day 18 C57BL/6 mice and N18TG2 neuroblastoma cells with morphological and cytoskeletal features similar to their neuronal precursors (Lee, Hammond, Large & Wainer, 1990). After differentiation with retinoic acid, HN9.10e cells give rise to action potentials upon membrane depolarization that resemble those recorded in slice cultures of the hippocampus and thus exhibit similar electrophysiological properties. In addition to a voltage-dependent Na^+ current and both transient ($I_{K(A)}$-type) and sustained outward potassium current ($I_{K(DR)}$-type), a membrane hyperpolarization-activated current was observed in a fraction of the cells. The activation range, kinetics and sensitivity to externally applied Cs^+ identified this current component as being related to a Q-type current (I_Q) previously described in hippocampal neurons (Halliwell & Adams, 1982; Colino & Halliwell, 1993), but not in other hybrid cells derived from neuroblastoma × glioma ancestors (Brown & Higashida, 1988). In these cell lines (e.g. NG108-15) there have been reported only well characterized outward K^+ currents, such as M-currents, delayed rectifier $I_{K(DR)}$-type, Ca^{2+}-activated K^+ currents (Brown & Higashida, 1988) and other slowly inactivating voltage-activated K^+ currents (Robbins & Sim, 1990).

* To whom correspondence should be addressed.

Analysis of HN9.10e currents indicated that in addition to an I_Q current, these hippocampal neurons displayed a second, and markedly different, current component in the negative voltage range. In order to molecularly define membrane hyperpolarization-activated currents better, we carefully investigated the functional properties of this slowly activating inward current component in HN9.10e cells. Our results indicate that this current is unlikely to be classified as a member of previously described ionic current families that are activated by membrane hyperpolarization, such as inwardly rectifying K^+ selective I_{Kir} currents and mixed cationic I_Q (I_H and I_F) currents.

METHODS

Mouse HN9.10e cells (a gift of Dr B. Wainer, Emory University, Atlanta, GA, USA) were cultured on glass coverslips in 35 mm Petri dishes at 37 °C and 5% CO_2–95% air in Dulbecco's modified Eagle's medium supplemented with 10% fetal calf serum, 2 mM L-glutamine, 0·1 mg ml^{-1} streptomycin, and 100 u ml^{-1} penicillin as described before (Lee *et al.* 1990; Glitsch, Wischmeyer & Karschin, 1996). For comparison of current characteristics, classic inwardly rectifying rat Kir2.1 channels were expressed in simian SV40 transformed COS-7 kidney cells (American Type Culture Collection (ATCC) no. CRL1650) using Lipofectamine as previously reported (Wischmeyer & Karschin, 1996).

Currents were recorded in the whole-cell, cell-attached and inside-out configurations of the patch-clamp technique (Hamill, Marty, Neher, Sakmann & Sigworth, 1981). Round phase-bright HN9.10e cells had capacitances between 15 and 25 pF. They appeared electrotonically compact with capacity transients that settled with a time constant of $< 800\ \mu s$, allowing adequate voltage-clamp conditions. The bath solution consisted of (mM): 135 NaCl, 5·4 KCl, 1·8 $CaCl_2$, 1 $MgCl_2$, 10 Hepes and 5 glucose; pH 7·4, adjusted with NaOH. The intracellular recording solution contained (mM): 140 KCl, 2 $MgCl_2$, 1 EGTA, 5 Hepes, 1 Na_2ATP and 0·1 cAMP; pH 7·3, adjusted with KOH. Alternative intracellular recording solutions were supplemented with Ca^{2+} and balanced with EGTA to yield concentrations of free Ca^{2+} between $\sim 10^{-12}$ M (0 $CaCl_2$ + 2 mM EGTA) and $\sim 10^{-5}$ M (1 mM $CaCl_2$ + 1 mM EGTA). A motor-driven fast microperfusion system with exchange rates of < 50 ms was used to perform local solution changes near the measured cell. All chemicals were obtained from Sigma (Deisenhofen, Germany); AFDX-348 was obtained as a gift from the Dr Karl Thomae GmbH, Biberach, Germany. Borosilicate pipettes were pulled and polished to give input resistances of 4–8 MΩ. Currents were measured at room temperature with a Heka (Lambrecht, Germany) EPC9 amplifier and low pass filtered at 1 (single channel data) or 2·9 kHz. Stimulation, series resistance compensation, data acquisition and analysis were performed using PULSE (Heka) and IGOR (WaveMetrics, Lake Oswego, USA) software on a Macintosh computer. Data are presented as means ± S.D. (with n as the number of cells).

RESULTS

Mouse embryonic hippocampus × neuroblastoma fusion cells (HN9.10e) expressed several ion channels typical of excitable cells under our culture conditions, such as voltage-dependent Na^+ channels, transient (K_A) and delayed rectifying potassium (K_{DR}) channels, as well as ionic conductances sensitive to both internal (K_{ATP}) and external ligands (5-HT3 receptor channels; e.g. Glitsch *et al.* 1996). In addition, different components of hyperpolarization-activated inward currents were identified in two distinct morphological variations of the cell line. A fraction of the flattened cells with elliptical cell bodies and arborized processes (5 out of 35 cells tested) expressed an inward current in response to hyperpolarizing voltage steps with first order activation kinetics. The activation time course was characteristic of I_Q/I_H currents, i.e. time constants of ~200 ms at a holding potential (V_h) of −100 mV which decreased with larger hyperpolarizations (McCormick & Pape, 1990; Fig. 1*A*). Application of 0·3 mM Ba^{2+} did not affect the amplitude of this current component (data not shown). Another fraction of HN9.10e cells, which was characterized by a round and bright cell body under phase contrast, was devoid of I_H currents. In these cells we discovered a prominent current component carried by K^+ ions that activated with anomalously slow kinetics upon hyperpolarization. Eighty-three out of 208 phase-bright HN9.10e cells measured in the whole-cell patch-clamp configuration developed a large inward current upon sustained hyperpolarization negative to a membrane potential of −80 mV, which we termed $I_{K(SHA)}$ (slow hyperpolarization-activated K^+ current; Fig. 1). With the extracellular K^+ concentration ($[K^+]_o$) elevated to 25 mM, $I_{K(SHA)}$ amplitudes averaged 750 ± 355 pA ($n = 12$) at $V_h = -120$ mV, which was equal to a current density of $37 \pm 16\ \mu A\ cm^{-2}$ membrane surface area. Based on its unique combination of activation potential, kinetics, cation permeability and external cation block this current was distinguishable from other known hyperpolarization-activated currents described so far (I_H, I_Q and I_F).

Activation and deactivation

When the membrane voltage was stepped to hyperpolarized potentials below −80 mV, $I_{K(SHA)}$ typically activated from a background inward current level of < -50 pA with (i) a characteristically long delay before the onset of current activation and (ii) a slow time course that differed significantly from the time course of I_H (Fig. 1*A* and *B*). In 5·4 mM external $[K^+]$ the activation potential of $I_{K(SHA)}$ was ~−70 mV, whereas I_H activated at slightly more positive potentials than −60 mV (Fig. 1*B*). For pulses between $V_h = -80$ and −140 mV the time course of activation determined from current onset varied widely between cells from a sigmoidal to an exponential waveform (fitted to a single exponential where possible) with time constants ranging from 900 to 3600 ms at −120 mV (1890 ± 770 ms, $n = 9$; Fig. 1*C*). In general, activation time constants of $I_{K(SHA)}$ varied between 1 and 7 s with smaller values for higher hyperpolarizations and were thus an order of magnitude slower than those for I_H (Fig. 1*D*). The unusually variable 'gating' behaviour of $I_{K(SHA)}$ led us to investigate whether the activation time depended on a diffusible

mediator, e.g. intracellular Ca^{2+} ions. However, change of either internal $[Ca^{2+}]_i$ from ~0 to 10 μM ($n = 5$; Fig. 1*C* inset) or internal $[Mg^{2+}]_i$ from 0 to 10 mM ($n = 7$; data not shown) had no significant effect on the activation time course, onset or amplitude of $I_{K(SHA)}$. As delay time we defined the time interval between application of voltage pulses and the point where the slope of current activation changed significantly (in less obvious cases > 20% of maximal slope). The delay time for pulses between $V_h = -80$ and -140 mV determined for twenty-six cells ranged from 1 to 10 s (e.g. $3{\cdot}7 \pm 0{\cdot}9$ s, $n = 9$ at $V_h = -120$ mV) and was linearly dependent on the applied membrane voltage when adequate recovery time (> 20 s) was allowed between voltage pulses (Fig. 2*A*). In the majority of cells $I_{K(SHA)}$ did not inactivate and remained at a sustained level during continuous hyperpolarizations between -80 mV and -140 mV. When the membrane voltage was repolarized during steady-state current activation to more positive potentials, $I_{K(SHA)}$ exponentially relaxed without significant delay with time constants that were independent of the new voltage level (Fig. 2*B*). Relaxation time constants (τ_{deact}) of tail currents were unique for each cell, but were significantly related to the activation time constant (τ_{act}; e.g. $\tau_{act} = 4380$ ms at -120 mV, $\tau_{deact} = 4200$ ms). The voltage dependence of steady-state deactivation of $I_{K(SHA)}$ could be described by a Boltzmann function with a half-maximal deactivation ($V_{½}$) at $-70 \pm 3{\cdot}9$ mV ($n = 4$; Fig. 2*C*).

Current–voltage relation and ion selectivity

The dependence of $I_{K(SHA)}$ activation on membrane hyperpolarization resulted in a steady-state current–voltage (*I–V*) relation that was strictly inwardly rectifying with no outward current and Ohmic slope conductance at hyper-

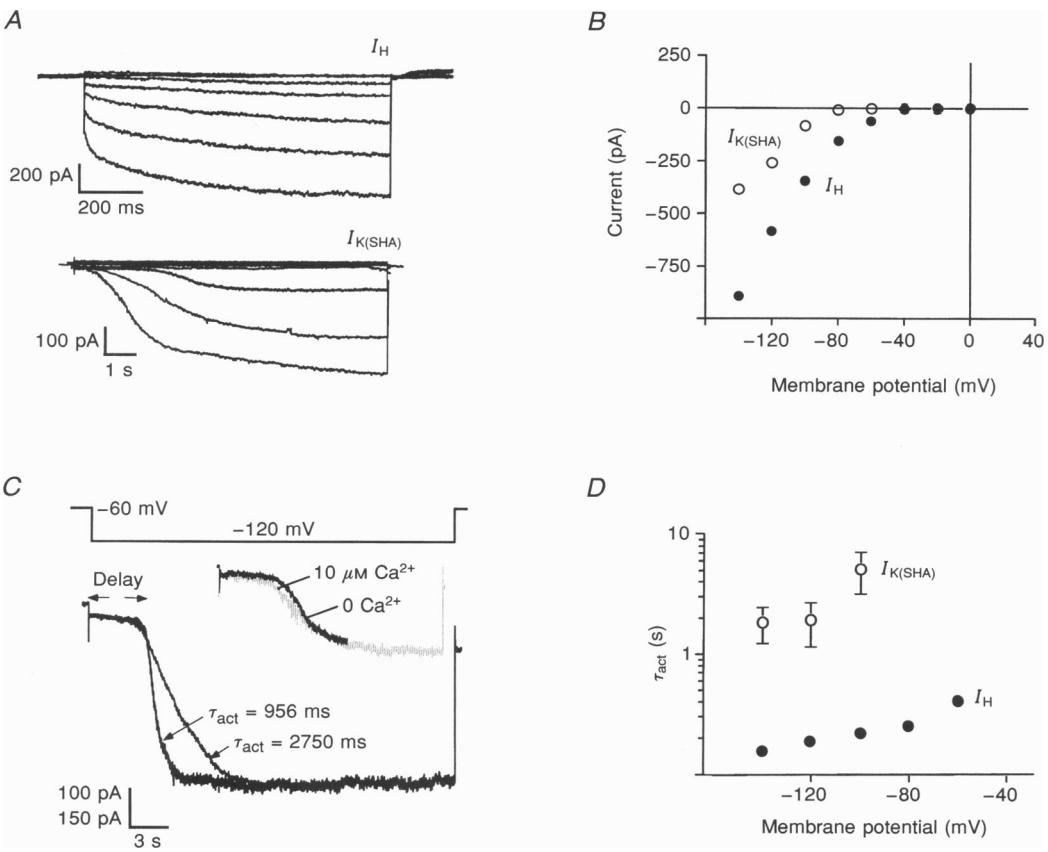

Figure 1. Hyperpolarization induces two types of inward current in HN9.10e cells

A, the upper panel shows whole-cell I_H currents of flat, phase-dark cells in 5·4 mM $[K^+]_o$ in response to hyperpolarizing voltage steps (1 s) ranging from 0 to -140 mV from a holding potential of -60 mV. In the lower panel $I_{K(SHA)}$ currents are recorded from round, phase-bright cells in response to longer hyperpolarizing pulses (10 s) from 0 to -140 mV from a holding potential of -60 mV. *B*, *I–V* plot of $I_{K(SHA)}$ and I_H currents shown in *A*, measured at the end of the voltage pulses. *C*, whole-cell recordings of $I_{K(SHA)}$ from two different cells in response to a 30 s hyperpolarizing pulse as indicated in the voltage protocol. $I_{K(SHA)}$ activates with a marked delay and variable time course (τ_{act} determined from single exponential fits). The inset shows whole-cell recordings of $I_{K(SHA)}$ from two different cells perfused with solutions containing ~0 (black trace) and 10 μM (grey trace) internal Ca^{2+} (see Methods). *D*, time constants (τ_{act}) determined from single exponential fits to the activation time course of $I_{K(SHA)}$ and I_H at different step potentials. Note the logarithmic scale of the ordinate.

polarized potentials beyond −70 mV. The 'activation' potential at which rectification occurred was independent of $[K^+]_o$ as would be characteristic of classic K^+ inward rectifiers (Kir; Fig. 3*A*). The steady-state activation curve showed a Boltzmann distribution with similar half-maximal activation potentials for 5·4 mM $[K^+]_o$ (−112 ± 2·3 mV; $n = 4$) and 25 mM $[K^+]_o$ (108 ± 2·4 mV; $n = 4$; Fig. 3*B*). This indicated that, in contrast to Kir channels, current activation is not strongly dependent on the difference $(V - E_K)$. The instantaneous open-channel *I–V* relation as determined from the tail current responses of $I_{K(SHA)}$ to repolarizing voltage steps in 5·4 and 25 mM $[K^+]_o$ was linear and revealed a current reversal potential close to the reversal potential for K^+ ions (E_K, Fig. 4*A*). The suggested high K^+ selectivity of $I_{K(SHA)}$ was also demonstrated by analysing open channel current in response to fast voltage ramps (420 mV s^{-1}), which was possible with little error due to the slow ($\tau > 4$ s) current relaxation time constants. Figure 4*B* and *C* shows ramp records obtained before and after hyperpolarizing the cells to −120 mV for 10 s (and monitoring $I_{K(SHA)}$ induction). The subtraction currents which were devoid of the majority of background conductances reversed at −71 ± 4·3 mV (5·4 mM $[K^+]_o$; $n = 7$; Fig. 4*B*), and −45 ± 5·1 mV (25 mM $[K^+]_o$; $n = 5$; Fig. 4*C*). The values were close to E_K as predicted from the Nernst equation, indicating that $I_{K(SHA)}$ was predominantly carried by K^+. Using this protocol, the *I–V* relation of $I_{K(SHA)}$ also revealed linearity of the current around E_K with slight rectification at more depolarized potentials.

In an additional set of experiments potassium ions in the external solution were replaced by other monovalent cations to test for their relative permeability: $I_{K(SHA)}$ channels were

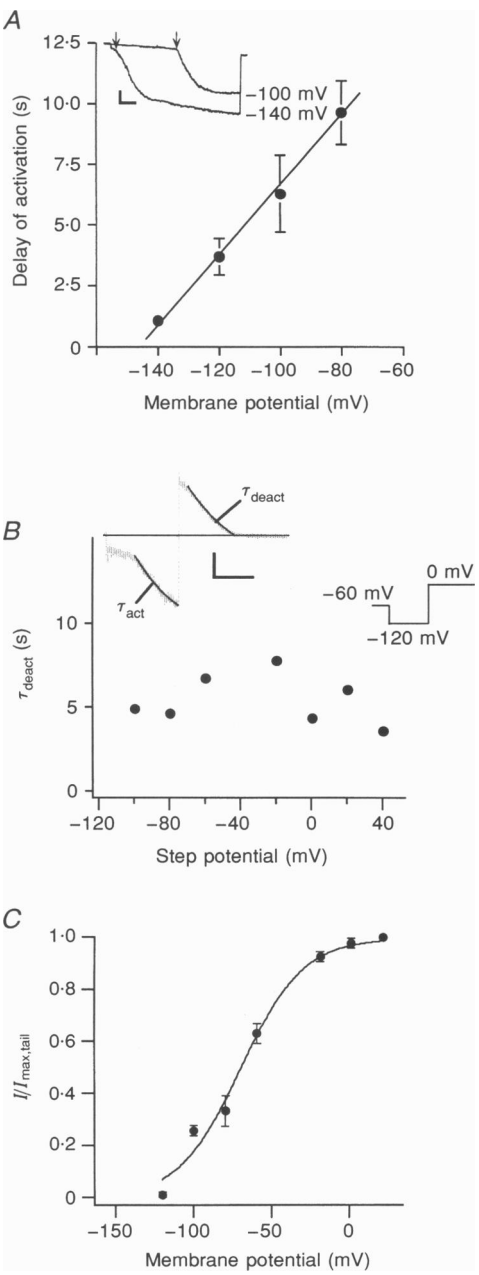

Figure 2. Delay in onset and deactivation of $I_{K(SHA)}$

A, mean delay time from the beginning of the voltage steps to the onset of current activation ($n = 7$) plotted against the applied membrane potential. The continuous line is a linear regression fit to the data. The inset shows current responses to voltages as indicated on the right; arrows denote the end of delay time; scale bars correspond to 100 pA and 2 s. *B*, time constants of $I_{K(SHA)}$ relaxation (τ_{deact}) plotted against the repolarizing potential to which the voltage was stepped back from a hyperpolarized potential of −120 mV. The inset shows a typical cell with similar $I_{K(SHA)}$ activation and relaxation time constants for a voltage step from −120 to 0 mV. Scale bars correspond to 50 pA and 2 s. *C*, the steady-state deactivation plotted against the membrane potential. Data are expressed as a fraction of the maximal tail current amplitude, $I_{max,tail}$, and are fitted to a Boltzmann function $[1/1 + \exp(V_0 - V_{½}/k)]$ with a midpoint, $V_{½} = -70 \pm 3{\cdot}9$ mV and a slope, $k = 19{\cdot}7 \pm 2{\cdot}79$ mV ($n = 4$) for every e-fold change in deactivation.

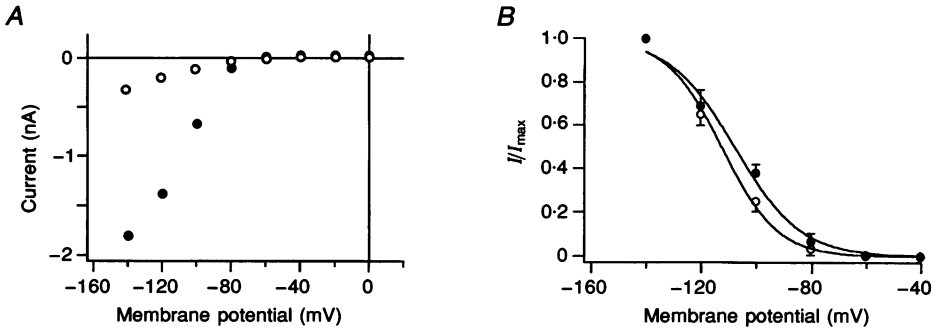

Figure 3. Steady-state activation of $I_{K(SHA)}$

A, current amplitudes in response to voltage steps between 0 and −140 mV reveal activation potentials of ~−75 mV and strong inward rectification for $I_{K(SHA)}$ in both 5·4 and 25 mM $[K^+]_o$. *B*, steady-state activation of $I_{K(SHA)}$ as the relative current amplitude I/I_{max} plotted *versus* the membrane potential in 5·4 mM (○) and 25 mM (●) $[K^+]_o$. A Boltzmann function (see Fig. 2*D*) was fitted to the data points with a midpoint, $V_{½} = -112 \pm 2$ mV and slope, $k = -10{\cdot}1 \pm 1$ for $[K^+]_o = 5{\cdot}4$ mM; and $V_{½} = -108 \pm 2{\cdot}4$ mV and $k = -10{\cdot}9 \pm 1{\cdot}2$ for $[K^+]_o = 25$ mM.

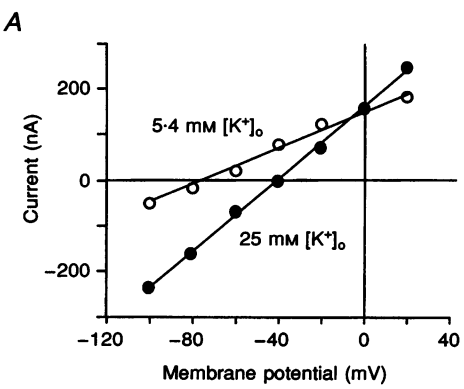

Figure 4. K^+ selectivity of $I_{K(SHA)}$

A, amplitudes of tail currents in 5·4 mM (○) and 25 mM (●) $[K^+]_o$ plotted against the repolarization potential ($V_h = -120$ mV). Currents reverse close to the Nernst potential E_K (~−75 mV for $[K^+]_o = 5{\cdot}4$ mM and ~−40 mV for $[K^+]_o = 25$ mM). *B*, thick traces denote a point-by-point subtraction of currents in response to 500 ms voltage ramps before (1) and after (2) steady-state activation (thin lines) of $I_{K(SHA)}$ through a conditioning hyperpolarizing pulse (see voltage protocol, upper panel) in 5·4 mM $[K^+]_o$. *C*, same experiment conducted in 25 mM $[K^+]_o$.

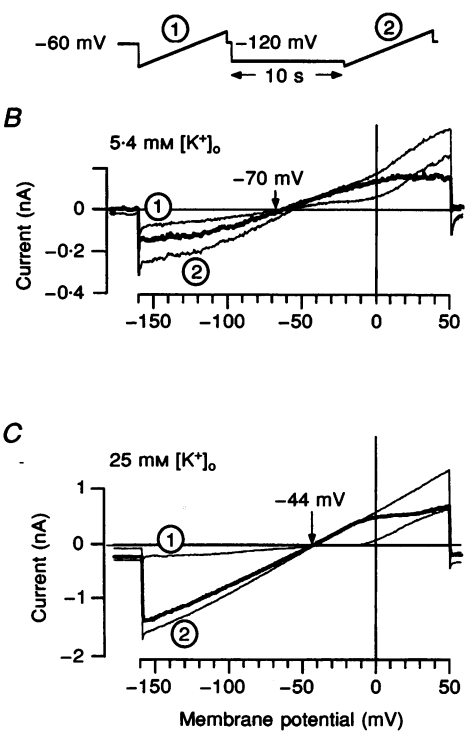

found to be impermeable to Na^+ and Rb^+, but slightly permeable to NH_4^+ (Fig. 5*A*, $n = 4$). Ramp recordings revealed reversal potentials of (mV): −98 for Na^+, −93 for Rb^+, −78 for NH_4^+ and −44 for K^+. As determined from the Goldman–Hodgkin–Katz equation under bi-ionic conditions, permeabilitiy ratios relative to K^+ were 0·24 for NH_4^+, 0·13 for Rb^+ and 0·11 for Na^+ (Fig. 5*B*).

Blockade by external cations

Extracellular Ba^{2+} and Cs^+ induce a time- and voltage-dependent channel block of both Kir channels and the hyperpolarization-activated channels underlying I_H. One millimolar Ba^{2+}, when externally applied by a rapid microperfusion system (< 50 ms) from the external side, also reversibly blocked $I_{K(SHA)}$, by 80 ± 12% ($n = 5$; $V_h = -120$ mV) with a rapid on and off rate ($\tau_{on} = 30$ ms; $\tau_{off} = 110$–190 ms; Fig. 6*A*). For comparison, the unique Ba^{2+} binding kinetics of recombinant Kir2.1 channels are superimposed in Fig. 6*A* with the characteristically slow unbinding of Ba^{2+} from the pore (τ_{off} ~4 s) as is typical of many inwardly rectifying Kir channels (Wischmeyer, Lentes & Karschin, 1994). Ramp recording of $I_{K(SHA)}$ shows a moderate increase in the efficiency of Ba^{2+} block at more depolarized potentials > 0 mV (Fig. 6*B*). The concentration–response relation revealed a K_i (i.e. the concentration producing 50% block) for Ba^{2+} of 420 μM which is an order of magnitude less sensitive than that of $I_{Kir2.1}$ (Fig. 6*C*). Similarly, a higher concentration of Cs^+ (5 mM) inhibited the current by 70 ± 9% ($n = 4$) with fast binding and unbinding of the blocking ion (time constants of 100–250 ms, Fig. 7*A*) that was only weakly dependent on the membrane voltage (Fig. 7*B*). The concentration–response relation for Cs^+ with a K_i of 2·77 mM is also an order of magnitude higher than that of $I_{Kir2.1}$ (Fig. 7*C*). Moreover, the block of $I_{K(SHA)}$ by Cs^+, but not Ba^{2+}, showed a characteristic 'rebound' effect which occurred repetitively and immediately upon removal of the blocker; i.e. the current transiently increased as channels unblocked and exponentially relaxed to its former amplitude with a time constant of 5360 ± 1370 ms ($n = 5$; Fig. 7*D*). In addition,

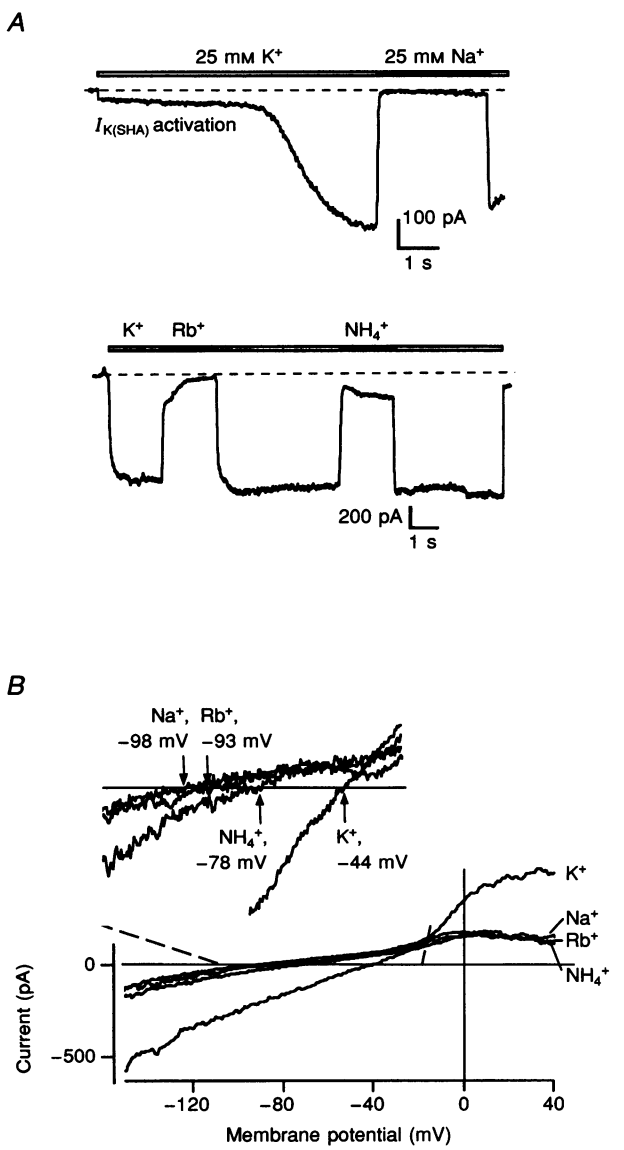

Figure 5. $I_{K(SHA)}$ is mainly carried by K^+

A, equimolar substitution for extracellular K^+ (25 mM) indicates that $I_{K(SHA)}$ channels are completely, or partially impermeable to Na^+ (top trace), NH_4^+ and Rb^+ (bottom trace). Dashed lines denote zero current levels. *B*, $I_{K(SHA)}$ currents in response to a fast voltage ramp (500 ms) reveal different reversal potentials for different monovalent cations under bi-ionic conditions (Na^+, −98 mV; Rb^+, −93 mV; NH_4^+, −78 mV; K^+, −44 mV). Permeability ratios were calculated according to the Goldman–Hodgkin–Katz equation, $pX/pK^+ = [K^+]_i/[X]_o \exp[(zV_{rev}F)/RT]$ with $[X]_o$ as the concentration of the permeant ion, and F, R and T having their usual meanings.

high concentration of Ca^{2+} (5 mM) inhibited $I_{K(SHA)}$ by 72 ± 7% ($n = 5$, data not shown).

The concentration–response relations demonstrated that $I_{K(SHA)}$ was less sensitive to Cs^+ than to Ba^{2+} with a K_i for Cs^+ at −120 mV that was 6·6 times larger than that for Ba^{2+}. These data contrast with both the values obtained for I_H, which exhibits a reversed Ba^{2+}/Cs^+ sensitivity (see Discussion), and I_{Klr}, which is more sensitive to both blockers by an order of magnitude.

Muscarinic inhibition

$I_{K(SHA)}$ was also subject to control by a signal transduction mechanism involving G protein-coupled receptors. In a subset of HN9.10e cells ($n = 8$) that had been stably transfected with human M2 muscarinic receptors, but not in wild-type cells, 1 μM ACh or muscarine selectively and reversibly inhibited $I_{K(SHA)}$. The agonist-induced suppression of $I_{K(SHA)}$ was half-maximal at a muscarine concentration of ~1 μM (K_i), occurred with an exceptionally fast onset ($\tau_{on} < 50$ ms), and relaxed with a slow and complex sigmoidal time course during the 2–3 s after removal of the agonist (Fig. 8*A*). Data from these cells indicated that the hyperpolarization-induced slow gating process of $I_{K(SHA)}$ developed in the presence of the M2 receptor agonist; however, it should be noted that the time course of $I_{K(SHA)}$ activation upon hyperpolarizing voltage steps ($\tau_{on,voltage}$) for a given cell was identical to the time course of recovery from block by muscarine ($\tau_{off,musc}$; Fig. 8*B*) at a given potential. Simultaneous application of muscarine and the selective M2 antagonist AFDX-348 (1 μM) abolished the blocking effect observed upon the sole application of muscarine (Fig. 8*C*).

$I_{K(SHA)}$ elementary currents

In addition to $I_{K(SHA)}$ channels, at the single channel level a population of 'K_{ATP}-type' channels with a conductance of 24 pS could be detected in some cell-free patches. These channels were in a conductance range that has been described for other members of this family (Ashcroft & Ashcroft, 1990) and in the inside-out patch configuration were completely and reversibly inhibited by 1 mM ATP in the extracellular (facing the inside of the membrane patch)

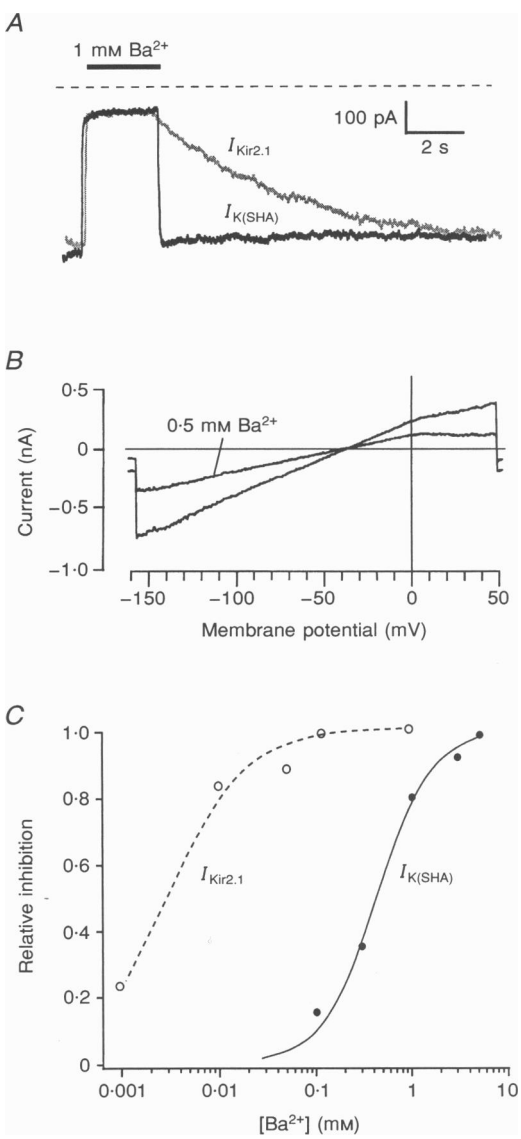

Figure 6. $I_{K(SHA)}$ is blocked by extracellular Ba^{2+}

A, extracellularly applied Ba^{2+} (1 mM) inhibits $I_{K(SHA)}$ (continuous traces) when steady-state activated at a potential of −120 mV. For comparison, block of recombinant Kir2.1 channels expressed in COS-7 cells has been superimposed (grey trace). Note the different time course of the unblocking reaction of Ba^{2+}, which is fast for $I_{K(SHA)}$ ($\tau_{off} = 110$ ms) and much slower for $I_{Kir2.1}$ ($\tau_{off} = 5340$ ms). *B*, after activation, $I_{K(SHA)}$ currents (as revealed by 500 ms ramp recordings) are inhibited by application of 0·5 mM Ba^{2+}. *C*, inhibition relative to block by a saturating concentration of Ba^{2+} is plotted *versus* the Ba^{2+} concentration (holding potential, $V_h = -120$ mV) for both $I_{K(SHA)}$ and $I_{Kir2.1}$ currents. Curves are least squares fits of data points to a Michaelis–Menten equation ($1/1 + [A/K_i]^n$) revealing a K_i of 0·42 mM for $I_{K(SHA)}$ (continuous line) compared with 0·05 mM for $I_{Kir2.1}$ (dashed line); A and n are variables.

solution (data not shown). Whole-cell analysis of $I_{K(SHA)}$ was thus generally performed with 1 mM ATP present in the internal solution to exclude a contribution from K_{ATP} channels. In the on-cell configuration single $I_{K(SHA)}$ channel activity, with a characteristic delay of $4{\cdot}55 \pm 1{\cdot}45$ s, could be observed in twelve out of thirty-eight patches following pulses to −120 mV (Fig. 9*A*). Although all of the patches contained more than one channel, elementary currents could reliably be measured at different hyperpolarizing potentials (Fig. 9*B* and *C*). The steady state *I–V* plot revealed inward rectification and a slope conductance of 7 ± 2 pS ($n = 5$) measured between −120 and 60 mV (Fig. 9*D*). After excision, channel activity persisted in inside-out patches (data not shown).

DISCUSSION

In mouse HN9.10e cells we have physiologically identified an inwardly rectifying K^+-selective current, $I_{K(SHA)}$, that slowly activated upon membrane hyperpolarization with complex kinetics and, to our knowledge, is unique in its combination of biophysical characteristics. Due to its very slow activation in the negative potential range beyond −80 mV, $I_{K(SHA)}$ could be analysed in almost complete separation from other intrinsic conductances that usually amounted to less than ~7% (~2·5 μA cm^{-2} membrane) of the average $I_{K(SHA)}$ current amplitudes.

Slow activation time course in response to hyperpolarizing command potentials is also characteristic of the inwardly rectifying cation current I_H (or I_Q) as well as the less well

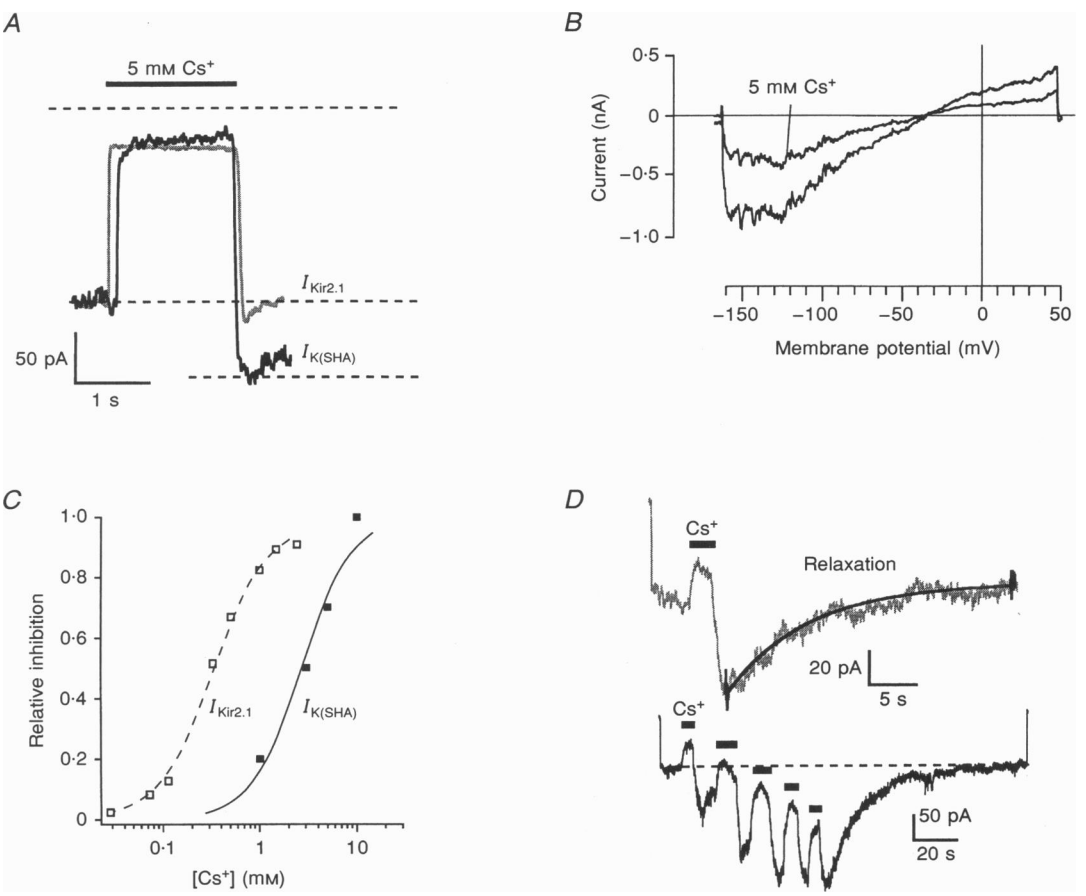

Figure 7. $I_{K(SHA)}$ is blocked by extracellular Cs^+

A, extracellularly applied Cs^+ (5 mM) inhibits $I_{K(SHA)}$ (continuous trace) when steady-state activated at a potential of −120 mV. For comparison, block of recombinant Kir2.1 channels expressed in COS-7 cells has been superimposed (grey trace). *B*, after activation of $I_{K(SHA)}$, application of 5 mM Cs^+ inhibits the current as depicted in fast voltage ramp recordings. *C*, inhibition relative to block by a saturating concentration of Cs^+ is plotted *versus* the Cs^+ concentration (holding potential, $V_h = -120$ mV) for both $I_{K(SHA)}$ and $I_{Kir2.1}$ currents. Curves are least squares fits of data points to a Michaelis–Menten equation ($1/1 + [A/K_i]^n$) revealing a K_i of 2·76 mM for $I_{K(SHA)}$ (continuous line) compared with 0·39 mM for $I_{Kir2.1}$ (dashed line). *D*, removal of Cs^+ causes a transient increase ('rebound') in $I_{K(SHA)}$ amplitude that relaxes to normal with monoexponential time course (top trace). Repetitive Cs^+ applications gradually increase $I_{K(SHA)}$ (bottom trace) to a transient peak level.

known hyperpolarization-activated K^+ currents $I_{K(H)}$ (Zittlau & Walther, 1991) and the Ba^{2+}- and Cs^+-insensitive $I_{K(AB)}$ (Araque & Buno, 1994), both identified in invertebrate skeletal muscle. I_H currents have been described in various central and peripheral neurons (Halliwell & Adams, 1982; McCormick & Pape, 1990; Akasu & Shoji, 1994), as well as in sino-atrial cells and Purkinje fibres of the heart (DiFrancesco, 1986), where they have been termed I_F. As also demonstrated in this report, these currents activate at potentials negative to −50 mV mostly with first order gating (alternatively described by the sum of two exponential components of opposite polarity; e.g. Hestrin, 1987) and time constants that are reduced with increased hyperpolarization, but usually are < 1 s. Another inward rectifier from canine hippocampus with first order gating, but slower activation constants resembles a 'classical' inward rectifier when expressed in *Xenopus* oocytes because activation depends on the extracellular K^+ concentration (Cui *et al.* 1992). $I_{K(SHA)}$, in contrast, exhibited complex activation kinetics that were highly variable between cells with activation time constants as slow as 7 s and a characteristic strongly voltage-dependent delay of 1–10 s (at −80 to −140 mV). Given that I_H, I_Q and I_F represent a molecularly homogeneous population of ion channels, their hallmark of selectively conducting both potassium and sodium cations would naturally exclude the purely K^+ selective $I_{K(SHA)}$ from this channel subfamily. An unusually small single channel conductance of ~1 pS (I_F; DiFrancesco, 1986) and the pharmacological profile likewise support separate channels species: I_H is only weakly affected by extracellular Ba^{2+} at even high concentrations (10 mM; Mayer & Westbrook, 1983; Spain, Schwindt & Crill, 1987; McCormick & Pape, 1990), whereas $I_{K(SHA)}$ was blocked by Ba^{2+} with a K_i of 420 μM. On the other hand I_H is markedly sensitive to a time- and voltage-dependent block by extracellular Cs^+, even more so than $I_{K(SHA)}$ (K_i = 2·77 mM), thus exhibiting reversed Ba^{2+}/Cs^+ sensitivity. Closer analysis of microperfused channel blockers reveals response characteristics distinctly different between the two channel types: in $I_{K(SHA)}$, for example, the current amplitude is transiently increased upon removal of Cs^+, but not Ba^{2+}. This 'rebound' effect has been described before in other

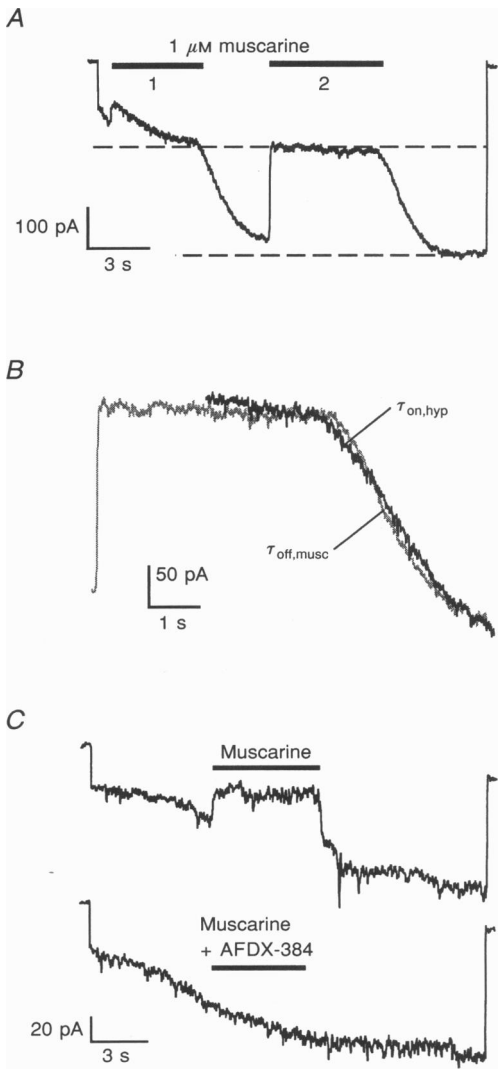

Figure 8. $I_{K(SHA)}$ is inhibited by muscarine

A, whole-cell recording of a HN9.10e cell stably transfected with the M2 muscarinic receptor in response to a −120 mV hyperpolarizing pulse. Muscarine (1 μM) was applied during the onset (1) and maintained (2) phase of $I_{K(SHA)}$. Dashed lines represent the levels of maximum $I_{K(SHA)}$ activation and steady-state block by 1 μM muscarine, respectively. *B*, time course of relaxation from muscarinic block ($\tau_{off,musc}$, grey trace) compared with the time course of activation of $I_{K(SHA)}$ by a hyperpolarizing pulse to −120 mV ($\tau_{on,hyp}$, black trace). *C*, inhibition of $I_{K(SHA)}$ by muscarine (1 μM) is abolished by simultaneous application of 1 μM of the specific M2 receptor antagonist AFDX-384.

ionophores, e.g. for the action of high pentobarbitone concentrations at $GABA_A$ receptors in dorsal root ganglion cells (Robertson, 1989) or for ACh acting at nicotinic receptors in adrenal chromaffin cells (Maconochie & Knight, 1992) and had been attributed to an overshoot current due to the removal of channel block.

The differential susceptibility to neuromodulators and downstream signalling components may also help to characterize $I_{K(SHA)}$. $I_{K(SHA)}$ was not significantly affected by alterations of the intracellular Ca^{2+} concentration, $[Ca^{2+}]_i$, between ~0 and 10 μM, whereas both amplitude and activation potential of I_F in sino-atrial node cells have been found to be dependent on $[Ca^{2+}]_i$ (Hagiwara & Irisawa, 1989; but see Zaza, Maccaferri, Mangoni & DiFrancesco, 1991). Similar to $I_{K(SHA)}$, however, but at much lower nanomolar concentrations, muscarinic agonists were found to rapidly ($\tau \approx 500$ ms) inhibit I_F in the same cells (DiFrancesco & Tromba, 1988; DiFrancesco *et al.* 1989), which is most likely to be via a direct, membrane-delimited action of activated G proteins (Yatani & Brown, 1990). These reports are in contrast to the modulation seen in hippocampal neurons where carbachol was found to both potentiate and accelerate the kinetic of I_Q (Colino & Halliwell, 1993).

Current suppression by muscarine has long been associated with the M current (I_M), a time- and voltage-dependent K^+ current that has been shown to exist also in neuroblastoma cells (NG108-15; Spain *et al.* 1987), but was originally found in frog sympathetic neurons and was the first current demonstrated to be under the negative synaptic control of acetylcholine (Brown & Adams, 1980). M currents are largely carried by K^+ ions, exhibit fairly long activation time constants (~150 ms at −35 mV) and lack time-dependent inactivation. However, they activate with steep voltage dependence upon depolarization and are fully closed at potentials more negative than ~−60 mV, a potential where $I_{K(SHA)}$ would barely start to activate; thus they more resemble delayed K^+ outward rectifiers (Constanti & Brown, 1981). In contrast to $I_{K(SHA)}$, M currents depend strongly on the concentration of free intracellular Ca^{2+}: elevation of $[Ca^{2+}]_i$ to 60 nM in bullfrog sympathetic neurons increases I_M amplitudes by a factor of two (Yu, 1995). This pronounced Ca^{2+} dependence may serve as another criterion to separate I_M from $I_{K(SHA)}$. In recent years the muscarinic

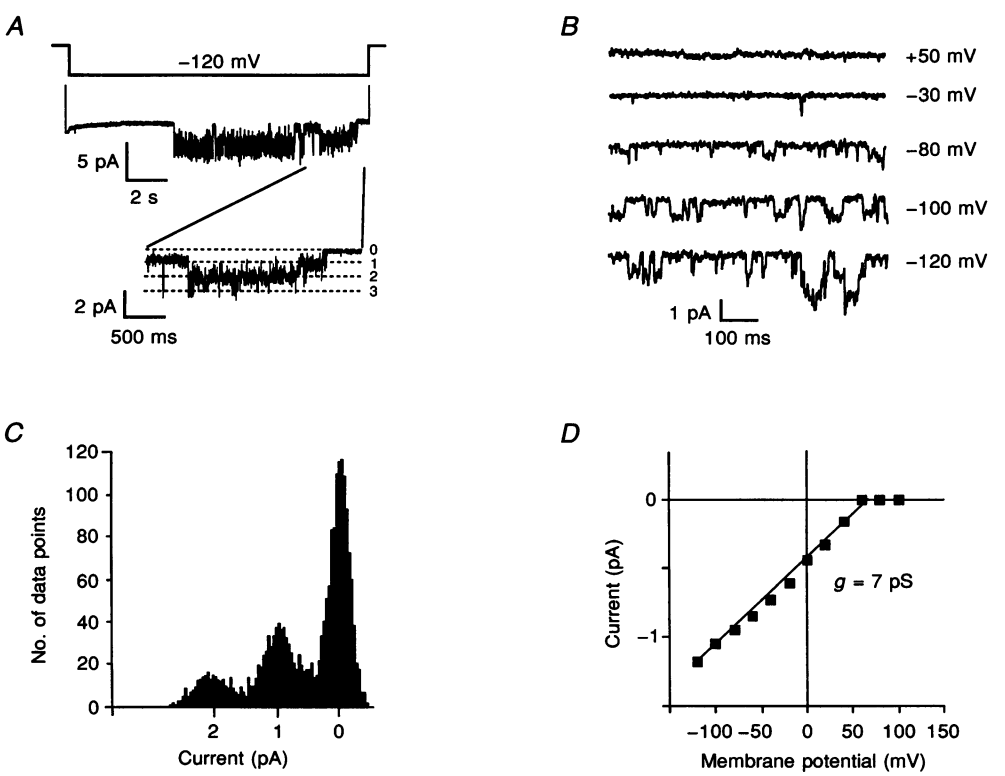

Figure 9. $I_{K(SHA)}$ elementary currents

A, $I_{K(SHA)}$ single channel activity in response to a hyperpolarizing voltage step to −120 mV occurs with the typical delay in onset (cell-attached configuration). *B*, single channel recordings of steady-state $I_{K(SHA)}$ activity in on-cell patches clamped to the potentials indicated at the right. *C*, amplitude histogram of $I_{K(SHA)}$ single channel events reveals current values for one and two open channels. The number of data points is plotted against the mean current flow per 0·75 ms bin at $V_h = -120$ mV. *D*, *I–V* plot of single $I_{K(SHA)}$ channels exhibits inward rectification and a slope conductance of 7 pS between −120 and 60 mV. All recordings were filtered at 1 kHz.

suppression of M channels, which (similar to I_H channels) are characterized by a small elementary conductance of 3–9 pS (Stansfeld, Marsh, Gibb & Brown, 1993), has been found to include the action of PTX-insensitive G proteins that may either act directly or via components of the PLC signalling cascade; either way the inhibition rate by muscarine had been found to be 10–20 min^{-1} (Lopez, 1992) and thus approximately two orders of magnitude slower than the muscarine inhibition of $I_{K(SHA)}$.

Is the muscarinic regulation indicative of classic inwardly rectifying K^+ (Kir) channels that are well known targets for G protein-mediated signalling cascades? Muscarinic inhibition via M1 receptors in fact has been observed to enhance excitability in neurons from rat sympathetic ganglia (Wang & McKinnon, 1996) and locus coeruleus (Shen & North, 1992). The recently established classification, molecularly and functionally, assigns Kir channels to three major subfamilies: mildly rectifying, ATP-sensitive Kir1.0 channels, Kir2.0 channels with strong rectification, and Kir3.0 channels, which are activated by receptor-activated $G_{\beta\gamma}$ subunits (Doupnik, Davidson & Lester, 1995). Although $I_{K(SHA)}$ is carried by K^+ ions, its steady-state I–V relation is strongly inwardly rectifying and the unitary conductance is only slightly smaller than that of small-conductance Kir channels, it fails to fulfil some of the other major requirements (Doupnik *et al.* 1995). Most importantly and in contrast to $I_{K(SHA)}$ (i) their activation potentials vary with E_K; (ii) channel 'gating' is fast and first order for Kir2.0 channels (activation and inactivation time constants ~1–10 ms at −100 mV; Wischmeyer *et al.* 1994) or proceeds with a slower bi-exponential time course in Kir3.0 channels (activation time constants between 50 and 400 ms; Kofuji, Doupnik, Davidson & Lester, 1996); and (iii) the instantaneous I–V relation is inwardly rectifying due to the voltage-dependent channel block by internal Mg^{2+} and nanomolar concentrations of positively charged polyamines (Ficker, Taglialatela, Wible, Henley & Brown, 1994; Fakler *et al.* 1994). Compared with $I_{K(SHA)}$, most classic Kir channels, exemplified by Kir2.1 in Fig. 6, are more sensitive to channel block by both Ba^{2+} and Cs^+ by at least one order of magnitude. Together with other blocker characteristics, such as the slow unbinding of Ba^{2+} from Kir2.1 channels that proceeds ~50 times slower, these data further support the uniqueness of $I_{K(SHA)}$.

Neurotransmitter-induced current inhibition with equally fast kinetics (< 1 s), mediated by muscarinic receptors and PTX-sensitive G proteins, has recently been described for strongly rectifying Kir channels in rat brain oligodendrocytes (Karschin, Wischmeyer, Davidson & Lester, 1994). In this respect it is highly intriguing that the muscarinic inhibition of $I_{K(SHA)}$ may eventually interfere with the channel's gating process as indicated by the identical kinetics of voltage-dependent current activation and recovery from inhibition after removal of the receptor.

The variable and unconventional gating behaviour of $I_{K(SHA)}$ also feeds speculations that the application of negative membrane potentials could relieve channel block by a mechanism that involves the binding or unbinding of internal messengers, such as G protein subunits. Like other K^+ inward rectifiers, $I_{K(SHA)}$ is likely to contribute to the maintenance of the neuron's resting potential, and strong (muscarinic) synaptic input that inhibits $I_{K(SHA)}$ may help to locally destabilize the membrane potential and make it vulnerable to the action of other incoming signals. The immortalized nature of the HN9.10e cell line together with the genetic manipulations possible will provide the opportunity to examine the nature of the putative signalling components and the molecular mechanism of $I_{K(SHA)}$ channel closure.

Akasu, T. & Shoji, S. (1994). cAMP-dependent inward rectifier current in neurones of the rat suprachiasmatic nucleus. *Pflügers Archiv* **429**, 117–125.

Araque, A. & Buno, W. (1994). Novel hyperpolarization-activated K^+ current mediated anomalous rectification. *Journal of Neuroscience* **14**, 399–408.

Ashcroft, S. H. & Ashcroft, F. M. (1990). Properties and functions of ATP-sensitive K-channels. *Cell Signaling* **2**, 197–214.

Brown, D. A. & Adams, P. R. (1980). Muscarinic suppression of a novel voltage-sensitive K^+ current in a vertebrate neurone. *Nature* **283**, 673–676.

Brown, D. A. & Higashida, H. (1988). Voltage- and calcium-activated potassium currents in mouse neuroblastoma × rat glioma hybrid cells. *Journal of Physiology* **397**, 149–165.

Cui, J., Mandel, G., DiFrancesco, D., Kline, R. P., Pennefather, P., Datyner, N. B., Has pel, H. C. & Cohen, I. S. (1992). Expression and characterization of a canine hippocampal inwardly rectifying K^+ current in *Xenopus* oocytes. *Journal of Physiology* **457**, 229–246.

Colino, A. & Halliwell, J. V. (1993). Carbachol potentiates Q currents and activates a calcium-dependent non-specific conductance in rat hippocampus in vitro. *European Journal of Neuroscience* **5**, 1198–1209.

Constanti, A. & Brown, D. A. (1981). M-currents in voltage-clamped mammalian sympathetic neurones. *Neuroscience Letters* **24**, 289–294.

DiFrancesco, D. (1986). Characterisation of single pacemaker channels in cardiac sino-atrial node cells. *Nature* **324**, 470–473.

DiFrancesco, D., Ducouret, P. & Robinson, R. B. (1989). Muscarinic modulation of cardiac rate at low acetylcholine concentrations. *Science* **243**, 669–671.

DiFrancesco, D. & Tromba, C. (1988). Inhibition of the hyperpolarization-activated current (i_f) induced by acetylcholine in rabbit sino-atrial node myocytes. *Journal of Physiology* **405**, 477–491.

Doupnik, C., Davidson, N. & Lester H. A. (1995). The inward rectifier potassium channel family. *Current Opinion in Neurobiology* **5**, 268–277.

FAKLER, B., BRÄNDLE, U., BOND, C., GLOWATZKI, E., KOENIG, C., ADELMAN, J. P., ZENNER, H. P. & RUPPERSBERG, J. P. (1994). A structural determinant of differential sensitivity of cloned inward rectifier K^+ channels to intracellular spermine. *FEBS Letters* **356**, 199–203.

FICKER, E., TAGLIALATELA, M., WIBLE, B. A., HENLEY, C. M. & BROWN, A. M. (1993). Spermine and spermidine as gating molecules for inward rectifier K^+ channels. *Science* **266**, 1068–1072.

GLITSCH, M., WISCHMEYER, E. & KARSCHIN, A. (1996). Functional characterization of two 5-HT3 receptor splice variants isolated from a mouse hippocampal cell line. *Pflügers Archiv* **432**, 134–143.

HAGIWARA, N. & IRISAWA, H. (1989). Modulation by intracellular Ca^{2+} of the hyperpolarization-activated inward current in rabbit single sinoatrial node cells. *Journal of Physiology* **409**, 121–141.

HALLIWELL, J. V. & ADAMS, P. R. (1982). Voltage clamp analysis of muscarinic excitation in hippocampal neurones. *Brain Research* **250**, 71–92.

HAMILL, O., MARTY, A., NEHER, E., SAKMANN, B. & SIGWORTH, F. (1981). Improved patch-clamp techniques for high resolution current recording from cells and cell-free membrane patches. *Pflügers Archiv* **391**, 85–100.

HESTRIN, S. (1987). The properties and function of inward rectification in rod photoreceptors of the tiger salamander. *Journal of Physiology* **390**, 319–333.

KARSCHIN, A., WISCHMEYER, E., DAVIDSON, N. & LESTER, H. A. (1994). Fast inhibition of inwardly rectifying K channels by multiple neurotransmitter receptors in oligodendroglia. *European Journal of Neuroscience* **6**, 1756–1764.

KOFUJI, P., DOUPNIK, C. A., DAVIDSON, N. & LESTER, H. A. (1996). A unique P-region residue is required for slow voltage-dependent gating of a G protein-activated inward rectifier K^+ channel expressed in *Xenopus* oocytes. *Journal of Physiology* **490**, 633–645.

LEE, H. J., HAMMOND, D. N., LARGE, T. H., ROBACK, J. D., SIM, J. A., BROWN, D. A., OTTEN, U. H. & WAINER, B. H. (1990). Neuronal properties and activities of immortalized hippocampal cells from embryonic and adult mice. *Journal of Neuroscience* **10**, 1779–1787.

LEE, H. J., HAMMOND, D. N., LARGE, T. H. & WAINER, B. H. (1990). Immortalized young adult neurons from the septal region: generation and characterization. *Developmental Brain Research* **52**, 219–228.

LOPEZ, H. S. (1992). Kinetics of G protein-mediated modulation of the potassium M-current in bullfrog sympathetic neurons. *Neuron* **8**, 725–736.

MACONOCHIE, D. J. & KNIGHT, D. E. (1992). A study of the bovine adrenal chromaffin nicotinic receptor using patch clamp and concentration-jump techniques. *Journal of Physiology* **454**, 129–153.

MCCORMICK, D. A. & PAPE, H. C. (1990). Properties of a hyperpolarization-activated cation current and its role in rhythmic oscillation in thalamic relay neurones. *Journal of Physiology* **431**, 291–318.

MAYER, M. L. & WESTBROOK, G. L. (1983). A voltage-clamp analysis of inward (anomalous) rectification in mouse spinal sensory ganglion neurones. *Journal of Physiology* **340**, 19–25.

ROBERTSON, B. (1989). Action of anaesthetics and avermectin on $GABA_A$ chloride channels in mammalian dorsal root ganglion neurones. *British Journal of Pharmacology* **98**, 167–176.

ROBBINS, J., MARSH, S. J. & BROWN, D. A. (1993). On the mechanism of M-current inhibition by muscarinic m1 receptors in DNA-transfected rodent neuroblastoma × glioma cells. *Journal of Physiology* **469**, 153–158.

SHEN, K.-Z. & NORTH, A. R. (1992). Muscarine increases cation conductance and decreases potassium conductance in rat locus coeruleus neurones. *Journal of Physiology* **455**, 471–485.

SPAIN, W. J., SCHWINDT, P. C. & CRILL W. E. (1987). Anomalous rectification in neurons from cat sensorimotor cortex in vitro. *Journal of Neurophysiology* **57**, 1555–1576.

STANSFELD, C. E., MARSH, S. J., GIBB, A. J. & BROWN, D. A. (1993). Identification of M-channels in outside-out patches from sympathetic ganglion cells. *Neuron* **10**, 639–654.

WANG, H.-S. & MCKINNON, D. (1996). Modulation of inwardly rectifying currents in rat sympathetic neurones by muscarinic receptors. *Journal of Physiology* **492**, 467–478.

WISCHMEYER, E. & KARSCHIN, A. (1996). Receptor stimulation causes slow inhibition of IRK inwardly rectifying K^+ channels by direct protein kinase A regulation. *Proceedings of the National Academy of Sciences of the USA* **93**, 5819–5823.

WISCHMEYER, E., LENTES, K. U. & KARSCHIN, A. (1994). Physiological and molecular characterization of an IRK-type inward rectifier K^+ channel in a tumour mast cell line. *Pflügers Archiv* **426**, 809–819.

YATANI, A. & BROWN, A. M. (1990). Regulation of cardiac pacemaker current If in excised membranes from sinoatrial node cells. *American Journal of Physiology* **258**, H1947–1951.

YU, S. P. (1995). Roles of arachidonic acid, lipoxygenases and phosphatases in calcium-dependent modulation of M-current in bullfrog sympathetic neuron. *Journal of Physiology* **487**, 797–811.

ZAZA, A., MACCAFERRI, G., MANGONI, M. & DIFRANCESCO, D. (1991). Intracellular calcium does not directly modulate cardiac pacemaker (i_f) channels. *Pflügers Archiv* **419**, 662–664.

ZITTLAU, K. E. & WALTHER, C. (1991). Hyperpolarisation slowly activates a potassium current in locust skeletal muscle. *Pflügers Archiv* **418**, 190–192.

Acknowledgements

We wish to thank D. Reuter for excellent technical assistance, Dr B. Wainer, Emory University, Atlanta, GA, USA, for making HN9.10e cells available to us, Dr J. Lai, Univeristy of Arizona, Tucson, AZ, USA for engineering stable M2 receptor transfectant cells, and the Dr Karl Thomae GmBH, Biberach, Germany for AFDX-348. We are also grateful to Dr C. Smith for critically reading the manuscript. This work was supported in part by grants from the Deutsche Forschungsgemeinschaft.

Author's email address

A. Karschin: akarsch@gwdg.de

Received 19 May 1997; accepted 15 July 1997.